Journal of the British Interplanetary Society, Vol. 37, pp. 124-134, 1984.

A PROPULSION-ORIENTED SYNTHESIS OF THE ANTIPROTON-NUCLEON ANNIHILATION EXPERIMENTAL RESULTS

GIOVANNI VULPETTI*
TELESPAZIO SpA per le Comunicazioni Spaziali, Via A. Bergamini 50, 00159 Rome, Italy.

The antiproton-proton and antiproton-neutron annihilation processes are reviewed in the light of recent experimental investigations. This paper is aimed at stressing those features that could be among the fundamental ones in conceiving an antimatter-matter powered spacecraft. Annihilation product mean-energy *versus* time diagrams are made for propulsion analysis purposes.

1. INTRODUCTION

The matter-antimatter annihilation process is recognised to be very attractive and promising for space propulsion [1-7]. An annihilation-based power source onboard a space vehicle, not necessarily a pure-rocket, would exhibit the highest energy density nowadays conceivable in a powerplant. Although the idea for utilising the annihilation process to propel spacecraft can be traced back to the early fifties [1], it is for less than a decade that investigations about a few of the several and the utmost challenging problems of an antimatter propulsion system have been performed in a systematic way [2-9]. Naturally, it is of basic importance to examine the properties and features of the prime candidate among the annihilation reactions potentially exploitable for space propulsion: the antiproton-nucleon annihilation at rest. The electron-positron annihilation is negligible on account of its low content of energy. The annihilation between an antiproton and a heavy nucleus is more complex than the antiproton-nucleon's. It might be used in very special circumstances to which we shall hint later. Finally, the general annihilation nucleus-antinucleus is deemed to be quite ruled out for a long time in the future (as it is apparent).

In Refs. 2 and 6 the energetics of the proton-antiproton annihilation at rest has been emphasised for space propulsion. The aims of this paper are several. First, to update the number and energy spectra characterising the proton-antiproton annihilation at rest. Second, to extend the above considerations to the antiproton-neutron at rest. Third, to stress whether the current knowledge about the nucleon-antinucleon annihilation at rest is sufficient for a (pre-) feasibility study of a space-borne propulsion system. Finally, to make energy *versus* time plots displaying the share, on the average, of the initial total mass (about two protons) among the primary and the secondary products of the annihilation reaction. Then, a possible generalisation of the admissible "operation points" first stressed by Cassenti [6] is suggested.

In the following we shall refer ourselves to some nuclear and particle physics concepts which are of basic importance in describing, though simply, the antiproton-nucleon annihilation. The complete definitions of such concepts and their physical meanings can be found in a great number of excellent textbooks. Here we have collected just a few of these for the convenience of the reader [10-17].

* Senior Scientist, Space Mission Analysis Division. The author points out that the topic of this paper is not connected with his duties at Telespazio.

2. EXPERIMENTAL PROCEDURES

We are chiefly interested in experiment here. Therefore, before going on to review the recent outcomes of the antiproton-nucleon ($\bar{p}N$) annihilation experiments, we spend a few words about some experimental procedures of data collection and analysis in certain branches of particle physics as the annihilation of hadrons. Our discussion will be based upon experimental facts.

When reaction products are to be recognised, one needs both targets and detectors, of course. One of the most used devices in particle physics is the bubble chamber where the liquid contained inside represents the target as well as the detector. Only charged particles can be revealed through the ionisation tracks they leave by interacting with the atomic electrons of the medium. Such paths are recorded by stereographic photos and processed by means of devices inputting information into a computer. Neutral particles cannot be detected unless they interact with the target's atoms in the visible chamber volume by production of some charged particles. Ionisation paths are detection-limited, in general. Tracks too short cause ambiguity and/or large experimental errors. Tracks too long tell nothing but the particles exited the detection chamber, namely, no stopping took place. A ionisation track is generally called a *prong*. The number and energy spectra of charged particles are measured by their characteristic prongs. If neutrals are involved in the reaction at hand, their spectra could be inferred quite indirectly from the conservation laws. Anyway, such spectra do generally suffer large errors due to the propagation of the direct experimental errors. An example of interest for us is represented just by annihilation measurements. Its study is generally accomplished by considering the reaction as follows:

$$a + \bar{a} \rightarrow xb + \text{anything}$$

The attention is focused on particles of type b, its number x, its energy (or momentum) spectrum and the total energy in the centre-of-mass frame (C.M.). "Anything" represents any other product(s). Such a methodology is called "inclusive study" [10]. By changing (the attention to) the particle b, the variety of the reaction characteristics should be covered. However, there are other significant policies of study. They support one another to give reliable experimental results.

The hadronic annihilation exhibits several products. It is not sufficient at all to apply the four-momentum conservation law to a specified number and type of particles in order to obtain their energy distribution. This is due to two reasons, substantially: the occurrence of additional conservation laws peculiar of the strong interaction (e.g. the strange-

ness and baryonic number conservation laws) and, largely, the number and type of steps through which the reaction proceeds (these considerations are not limited to the annihilation reactions, of course). To shortly clarify the latter point, let us consider the reactions

$$a + b \rightarrow d + e + c \qquad (1a)$$

$$a + b \rightarrow R + c \qquad (1b)$$
$$\hookrightarrow d + e$$

The two reactions exhibit the same initial and final particles. The initial total four-momentum in (1a) equals (1b)'s and so forth. However, whereas (1a) is a pure three-body reaction, (1b) takes place in two steps: at first the resonance R is formed. R is a very-short-life particle not directly observable by a prong (even though it can be charged). It decays, in our example, into two long-life particles d and e which are actually observed. The final energetics in (1a) is quite different from the (1b)'s. In fact, in a kinetic energy space such as the Dalitz plot [10] the energy of d, e and c in (1a) is uniformly distributed in the (a, b) C.M. In contrast, the reaction (1b) proceeds *via* two two-body steps. As a consequence, in the (a, b) C.M. the c's energy is fixed. In addition, in the R's C.M. both d and e have their own fixed energy according to the well-known two-body decay energy sharing. If we envisage that several a and b particles interact at a prefixed energy in their C.M., and the probabilities of the branches (1a) and (1b) are not negligible with respect to each other, then the energies of d, e, c in the (a, b) C.M. consist of bands and peaks. For instance, if c=e the mean energy of the particle c depends upon the branching ratio between (1a) and (1b), the R's mass and, naturally, the initial available reaction energy. These brief considerations can be extended to much more complex reactions involving more than three particles and/or more than one resonance. The $\bar{p}N$ annihilation reaction has been experimentally found to exhibit several branches and many resonances, as we shall see in the next sections.

3. THE ANNIHILATION ENVIRONMENT

For possible space propulsion applications the $\bar{p}N$ annihilation must occur at rest. By this phrase we mean that the initial $\bar{p}$'s momentum (relative to the nucleon which can be assumed at rest in the ship frame) should be, say, below ~50 MeV/c. This entails that the $\bar{p}$'s kinetic energy would be ~1 MeV at most. One should think, in fact, of transportation problems on-board. Anyway, the antiprotons must pass through a certain amount of matter, lose their energy and thereafter annihilate. The last step is not a simple thing. Here we limit ourselves to describing some consequences of interest in this paper.

Most of the present-day understanding of the antiproton-nucleon dynamics comes from analyses of photos from bubble chambers. However, in such devices statistics are generally limited and the initial atomic state of the $\bar{p}N$ annihilation (see below) can only be inferred, not measured directly. A sufficiently high statistical level is required to precisely "allocate" the great number of resonant and non-resonant states observed in the $\bar{p}N$ annihilation. On the other hand, to know the $\bar{p}$-p or $\bar{p}$-d atom's initial-state quantum numbers is basic in order to remove to a large extent the difficulties about the different annihilation channels delivering to a certain final product state. Studies are still in progress by particle physicists collaborations to clarify several points in $\bar{p}N$ annihilation at rest. They aim at using a new facility at CERN, namely, the *L*ow-*E*nergy *A*ntiproton *R*ing (LEAR) [18].

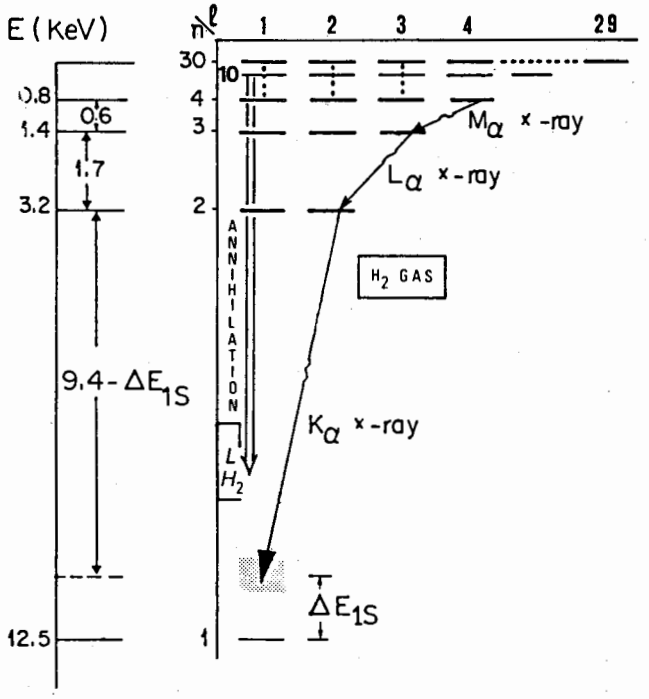

Fig. 1. Energy levels of the protonium ($\bar{p}$-p atom). In a liquid molecular target such as the bubble chamber H_2 the collisional Stark mixing effect populates the S-levels with high principal quantum number. These levels decay chiefly *via* annihilation. P-wave annihilations are very rare. In gaseous hydrogen at low pressure the situation can be quite different. This foresight, if confirmed by experiments at CERN, could be a result of great importance for space applications.

In this paper we will try to synthesise the amount of data from bubble chambers for potential space applications.

Generally, a bubble chamber is filled with liquid H_2 (or D_2). When an antiproton is stopped there, an H atom captures it by its Coulomb field. (Here stopping and capturing mean that the antiprotons have been slowed-down to a few eVs in energy and their impact parameter with respect to the H-atom's proton is about the classical radius of the K-shell). But the system (p, e^-, $\bar{p}$) is unstable and partially de-excites by emitting the electron. The remnant system is very important: it is called antiprotonic hydrogen or, more simply, *protonium*. The protonium's energy levels correspond to the ordinary H's. However, the Rydberg constant is scaled up by the factor $m_p/2m_e$ (m_p = proton mass, m_e electron mass). The Lyman and Balmer series, for instance, fall into the soft X-ray region, whereas the maximum binding energy is about 10 KeV (Fig. 1). The capture of an antiproton takes place in high-n (n = principal quantum number) orbitals. Although capturing is by the proton's Coulomb field, the protonium can be considered a pure Quantum-Electro-Dynamics (QED) system *only* in very external orbitals such as the capture's (there, typically n=30). In lower states the *strong* interaction between p-$\bar{p}$ adds to the Coulomb potential. This strong potential is responsible for a shift and broadening of the protonium energy levels. The excited protonium decay towards lower energy states. However, an important effect dominates such a de-excitation. In vacuum (ideal environment) a high-n would entail a corresponding high angular momentum by electric dipole transition. In real environments such as the bubble chamber's, the protonium experiences the intense Coulomb fields produced by the neighbouring hydrogen atoms. In other words, the Stark effect mixes the degenerate states and, in particular, provides the S-state for a non-negligible probability. In addition, it is known from Quantum

Mechanics that under the Stark effect the selection rules for atomic transitions are not strict; otherwise forbidden transitions can take place. All this can ultimately result in a large population in the S-states before the annihilation – $^1S_0$ and $^3S_1$ – (according to the spectroscopy notation), for which the principal quantum number is still rather high.

The next step consists of the annihilation which, therefore, takes place largely in high-n S-wave states. The probability of annihilation in such conditions is rather high because the S-orbital wave function exhibits a non-negligible value at the origin. In particular, detailed calculations indicate that the Stark effect in liquid H_2 is responsible for a "shuffling" of the degenerate states of angular momentum in protonium such that the S-wave annihilation should be many orders of magnitude more probable than the P-wave's for n-values down to ten [18]. As a consequence, these facts turn to high values of the annihilation cross section at low $\bar{p}$'s energy. We shall return to the annihilation-at-rest cross section data later on.

The above discussion is substantially what is meant by annihilation at rest in a bubble chamber. Among many complex things, annihilation is in reality an environment-dependent process. Following the current ideas, we shall assume throughout this paper that the bulk of experimental data largely come from S-wave annihilations. We neglect P-wave contributions. Details about antiprotonic atoms, annihilation and special states called "baryonium" can be found in [18-22].

Appropriately analogous remarks can be made for the $\bar{p}$-d atoms.

Some considerations oriented to space propulsion are in order. As we have seen above, the annihilation process follows or is in competition with X-ray emission. In a "realistic" matter-antimatter annihilation engines there would be a high number of annihilations per time unit inside the "annihilation chamber" which delivers the total energy-for-thrusting to the nozzle. Something like 10^{20} to 10^{21} annihilation/sec may be necessary for a *fast* interplanetary flight and even more for interstellar travel, even though to nearby stars. If the engine is designed to operate at low-thrust and high-specific-impulse, then relativistic particles are to be ejected. This can occur, for example, if the fluxes of matter and antimatter (not necessarily equal to each other) mixed together for reacting form a low-density "cloud" from which the high energy particles gush out. The very abundant "rain" of X-rays from the protonium cascades impinges upon the structure around the annihilation chamber or is absorbed by the "annihilation plasma," thus raising its temperature. In any case a hot sphere radiates over the whole solid angle. However, this unavoidable environment may be turned into an advantage, at least partially. By suitably designing the engine, absorbers in the ultraviolet/soft-X-ray range might recover an otherwise lost amount of energy. Such a quantity is quite negligible with respect to the propulsion energy, but it may be a very appreciable amount for supplying payload power, generating electromagnetic fields, feeding several control devices, processing data on-board, telemetry and so forth. On the other hand, the annihilation-at-rest process in environments so different from a bubble chamber may reveal new aspects from both the theory and application viewpoints. In these perspectives the experiments in progress at LEAR [18] using gaseous hydrogen are quite important. Naturally, as said above explicitly, the current bulk of information comes from bubble experiments and we keep on reviewing them in this paper.

4. THE ANTIPROTON-PROTON ANNIHILATION AT REST

In this section we describe the type, the mean number and the mean energy of the particles following the proton-antiproton ($p\bar{p}$) annihilation at rest. We distinguish primary and secondary products of annihilation.

4. 1 Primary Products

The $p\bar{p}$ annihilation-at-rest reaction can be formally written

$$p + \bar{p} \rightarrow rR + \underline{n}\cdot\underline{\pi} + \underline{\alpha}\cdot\underline{K} + \underline{\beta}\cdot\underline{\bar{K}} \qquad (2)$$

where the upper bar denotes an antiparticle and $\rightarrow$ denotes a strong interaction. According to the isospin multiplicity we have defined the following vectors:

$$\underline{\pi}^T = [\pi^+ \pi^- \pi^\circ], \underline{K}^T = [K^+ K^\circ], \underline{\bar{K}}^T = [K^- \bar{K}^\circ] \qquad (3)$$

where π and K denote pions and kaons respectively. The superscripts $\pm$ ° indicate their charge. The nomenclature used is standard in particle physics; our vector notation in Eq. (2) is for ease here. In addition, r, $\underline{n}$, $\underline{\alpha}$ and $\underline{\beta}$ represent the number of the corresponding particles in the reaction, the symbol R denoting a resonance.

Resonances establish some main branches and the steps through which the reaction actually takes place (Section 2). When $r > 0$ the number of prongs detected in the laboratory (LAB) is not generally given by the sum of the charged components of $\underline{n}$, $\underline{\alpha}$ and $\underline{\beta}$. In fact, R can decay into pions and/or kaons. Also, the charge balance of the righthand side of Eq. (2) accounts for the R's charge; R can be a multiplet of isospin too.

In general, in particle physics the resonances are grouped in meson and baryon resonances. In the $p\bar{p}$ annihilation at-rest no baryon resonance is possible by the simultaneous energy and baryonic-number conservation laws. In contrast to the resonance concept, we must report that particle physicists define as stable those particles immune to decay *via* the strong interaction (for instance, the meson π° which lives about 100 attoseconds is considered a stable particle). With these considerations in mind, what experimentally appears are the total number of pions and kaons *directly* produced and *coming* from the decay of the involved resonances. This sentence does not exclude R from decaying in other types of particles. (In fact, meson resonance can yield products such as photons, leptons or other meson resonances too). Four things are of major interest for the purposes of this paper: (1) the mean number of charged and neutral pions; (2) the mean numbers of charged and neutral kaons; (3) their mean energy; (4) the mean energy of non-π and non-K products from the R's decay and their branching ratio. Points 1-2 represent the output of inclusive studies on pions and kaons.

In order to understand the experimental results, let us first consider the resonances revealed in $p\bar{p}$ annihilations and their major decay modes. The following meson resonances have been found in the $p\bar{p}$ annihilation at rest:

$$(1)\rho\ (0)\omega\ (0)\eta'\ (1)B\ (0)f\ (1)A\ (1)A_2 \qquad (4)$$

listed in order of increasing mass. The isospin value has been reported in parenthesis. Complete information about the quantum numbers of the Rs in Eq. (4) can be found in Ref. 27. There are other resonances in the $p\bar{p}$ annihilation; however, their occurrence is quite low and will not be considered here. The resonances listed in Eq. (3) decay largely by strong interaction. There is another important particle which experimentally appears as a peak, but it does not decay strongly: the boson η (isospin singlet). It is responsible for a non-negligible contribution of pions and gammas from its decay. Such short-life particles are formed by the energy available in $p\bar{p}$ C.M., namely, about 1877 MeV. They all

appear in the pionic final states of the $p\bar{p}$ annihilation. The major contribution to such states comes from the resonances ρ and ω (see [18]). The remaining resonances can decay into ρ and ω and pions with a high probability among their own admissible decaying modes. The dominant decaying modes of ρ, ω and η are as follows:

$$\rho^+ \to \pi^+ + \pi^\circ, \rho^- \to \pi^- + \pi^\circ, \rho^\circ \to 2\,\pi^\circ \qquad (5)$$

$$\omega \Rightarrow \begin{cases} \to (\pi^+ + \pi^- + \pi^\circ & (90\%) \\ \Rightarrow \pi^\circ + \gamma & (8.7\%) \\ \Rightarrow \pi^+ + \pi^- & (1.3\%) \end{cases} \qquad (6)$$

$$\eta \Rightarrow \begin{cases} 2\,\gamma & (39\%) \\ 3\,\pi^\circ & (32\%) \\ \pi^+ + \pi^- + \pi^\circ & (24\%) \\ \pi^+ + \pi^- + \gamma & (5\%) \end{cases} \qquad (7)$$

where $\Rightarrow$ denotes electromagnetic interaction, as usual in particle physics. Leptonic modes are quite negligible in occurrence frequency. Some considerations are in order.

No dominant annihilation state pertains to leptonic components, in particular neutrinos. As a consequence, the *first two* steps in the $p\bar{p}$ annihilation are full-energy steps from a potential propulsion energy budget standpoint. All kaons of the reaction $p\bar{p}$ are produced directly; in fact, the "emission" of K-mesons from the resonances (4) is quite negligible. We shall see next that final states containing kaons are somewhat less probable than the ones containing pions only. Nevertheless, their role in conceiving an antimatter-matter engine should not be neglected as we will mention later.

From what is described above, the *primary* products from the $p\bar{p}$ annihilation are largely pions, a little contribution of kaons and a negligible amount of photons and leptons. We can re-write the reaction (2) as follows:

$$p + \bar{p} \to \underline{N} \cdot \underline{\pi} + \underline{\alpha} \cdot (\underline{K} + \underline{\bar{K}}) \qquad (8)$$

where $\| \underline{\alpha} \| \ll \| \underline{N} \|$. A key-point for a propulsion-oriented analysis consists of the mean values of $\underline{N}$, $\underline{\alpha}$ and the mean energy of the components of $\underline{\pi}$ and $\underline{K}$. Such values depend upon the annihilation environments and the resonant and non-resonant interaction modes through which the antiprotonic hydrogen atoms pass, as discussed above.

The average values we are going to write update the old data given in Ref. 23. Details about the current number spectra of pionic and kaonic states can be found in Refs. 18, 24, 25, 26. We have for the *averaged* spectra of the pion and kaon final states respectively:

$$\begin{aligned} &N^+ = N^- = 1.527 \pm 0.019 \\ &N^\circ = 1.96 \pm 0.23 \\ &E_\pi^+ = E_\pi^- = 374 \text{ MeV} \\ &E_\pi^\circ = 358.5 \text{ MeV} \\ &N^+ + N^- + N^\circ = 5.01 \pm 0.23 \\ &\alpha^+ = \alpha^- = 0.012 \\ &\alpha^\circ = \bar{\alpha}^\circ = 0.013 \end{aligned} \qquad (9)$$

$$\begin{aligned} &E_K^+ = E_K^- = 633 \text{ MeV} \\ &E_K^\circ = E_K^\circ = 633 \text{ MeV} \\ &\alpha^+ + \alpha^- + \alpha^\circ + \bar{\alpha}^\circ = 0.050 \pm 0.006 \end{aligned} \qquad (10)$$

The set of values in Eq. (10) have been estimated by the author on the basis of detailed partial-rate tables of extensive experiments performed at CERN and Columbia University [18]. Nevertheless, we must notice that several channels or final states including kaons are very difficult to analyse experimentally. These states, which are likely to occur because the system $p\bar{p}$ is an eigenstate of the charge conjugation operator, have not been reported in the literature. Therefore, the actual mean number of kaons is presumably underestimated. In Eq. (10) we have assumed $E_K^\pm = E_K^\circ$ for simplicity (and lack of information too). The distributions of both neutral pions and kaons are rather large; in contrast, the charged pions distributions are narrow because measured directly.

We can then summarise the relations (2) through (10) as follows: mean $p\bar{p}$ annihilation at rest (in liquid hydrogen)

$$p + \bar{p} \to 1.527\,\pi^+ + 1.527\,\pi^- + 1.96\,\pi^\circ + 0.012\,K^+ + 0.012\,K^- + 0.013\,K^\circ + 0.013\,\bar{K}^\circ \qquad (11)$$

which should represent a $p\bar{p}$ baseline for our next studies on matter-antimatter engines and mission profiles at the present-day knowledge. For we read the reaction (11) in terms of "produced" rest mass (M), massive particle kinetic energy (KE), gamma energy (GE) and neutrino energy (NE):

$$M = 715.6 \text{ MeV} \quad KE = 1161 \text{ MeV} \quad GE = 0 \quad NE = O \qquad (12)$$

Neutrinos are considered zero-mass particles. They do not contribute to the propulsion energy in any case.

As qualitatively described in the Introduction, the time evolution of the above parameters is one of the main goals of this paper. The values (12) undergo a significant change after about 10^{-16} seconds (or 100 attoseconds) since the annihilation time, a long time indeed; for comparison, the characteristic time of the η-meson (which lives much more than the resonances listed in Eq. (4) is less than a atto-second.

4. 2 Secondary Products and Chain Decays

Pions and kaons, although defined as stable particles (see Section 3), decay. As far as their meanlife-at-rest (MLAR) is concerned, we can distinguish different scales of time. The charged components have the following MLARs [27]:

$$\pi^\pm : 26.030 \text{ nanosec} \qquad K^\pm : 12.371 \text{ nanosec} \qquad (13)$$

These meanlives are dilated in LAB by the appropriate Lorentz factors. From reaction (11) we compute

$$\pi^\pm : 69.753 \text{ nanosec} \qquad K^\pm : 15.863 \text{ nanosec} \qquad (14)$$

or, in terms of mean distance travelled before decaying in LAB,

$$\pi^\pm : 19.4 \text{ m} \qquad K^\pm : 2.98 \text{ m} \qquad (15)$$

The neutral pion exhibits a MLAR equal to

$$\pi^\circ : 83 \text{ attosec} \qquad (16)$$

dilated in LAB (Reaction 11 again):

$$\pi^\circ : 220.5 \text{ attosec} \qquad \pi^\circ : 610 \text{ Å} \tag{17}$$

Neutral kaons are particular particles. A beam of K° (or $\bar{K}^\circ$ or both) can be thought to be composed of two states named K_S° and K_L° with equally-shared intensity. The subscripts 'S' and 'L' stand for 'short' and 'long' respectively because of the different MLARs such states characterise. Details about the neutral kaon can be found, for instance, in Ref. 10. From [27] we extract

$$K_S^\circ : 0.08923 \text{ nanosec} \quad K_L^\circ : 51.83 \text{ nanosec} \tag{18}$$

whereas we obtain in LAB

$$K_S^\circ : 0.1135 \text{ nanosec} \quad K_L^\circ : 65.92 \text{ nanosec} \tag{19}$$

$$0.02 \text{ metres} \qquad 12.21 \text{ metres} \tag{20}$$

The time scales translated into distance scales then result in the following practical values

$$\begin{aligned} &(\pi^\circ, K_S^\circ) \sim \text{null path} \quad K^\pm \sim 3 \text{ metres} \\ &K_L^\circ \sim 12 \text{ metres} \quad \pi^\pm \sim 20 \text{ [30] metres} \end{aligned} \tag{21}$$

where the value in brackets accounts for the $\pi^\pm$ from the kaonic decay.

To see how the values (12) evolve with time according to the temporal scales just mentioned, we examine the major decay modes of pions and kaons. From Ref. 27 we report:

$$\begin{aligned} &\pi^+ \to \mu^+ + \nu \qquad (100\% \text{ decay branching ratio}) \\ &\pi^\circ \to 2\gamma \qquad (98.8\%) \\ &K^+ \to \mu^+ + \nu \qquad (63.5\%) \\ &\qquad \pi^+ + \pi^\circ \qquad (21.2\%) \\ &\qquad (15.3\% \text{ for 3-body pionic, leptonic and rare decays}) \\ &K_S^\circ \to \pi^+ + \pi^- \qquad (68.6\%) \\ &\qquad 2\pi^\circ \qquad (31.4\%) \\ &K_L^\circ \to 3\pi^\circ \qquad (21.5\%) \\ &\qquad \pi^+ + \pi^- + \pi^\circ \ (12.4\%) \\ &\qquad \pi^\pm + \mu^\mp + \nu \ (27.1\%) \\ &\qquad \pi^\pm + e^\mp + \nu \ (38.7\%) \end{aligned} \tag{22}$$

The decays of π^-, K^- and $\bar{K}^\circ$ are straightforward obtained by the charge conjugation operation. In reactions (22) we made no distinction between neutrino-μ and neutrino-e (and their respective antiparticles) because this is not necessary for the aims of this paper. The energy sharing in the two-body decays is easily calculated (in the case of π° there is a frequency shift for the two gammas in LAB; only the mean energy will concern us).

From the pion decay:

$$E_\mu^\pi = 294 \text{ MeV} \quad E_\nu^\pi = 80 \text{ MeV} \quad E_\gamma^\pi = 179 \text{ MeV}$$

From the kaon decay (non K_L° events):

$$E_\mu^K = 331 \text{ MeV} \quad E_\nu^K = 302 \text{ MeV}$$

$$E_\pi^K = 316.5 \text{ MeV} \quad E_\gamma^K = 158 \text{ MeV (successive } \pi^\circ \text{ decay)}$$

As far as the three-body decay of K_L° is concerned, because $(m_{\pi'\mu'e}/m_{K^\circ})^2 \ll 1$ and the many decay channels involved we assume a product's energy mean value equalling one-third of the K_L° energy

$$E_{\pi'\mu'e'\nu} = 211 \text{ MeV}$$

In order to obtain the energy sharing at the successive decay times, we must take into account both the branching ratios in (22) and the number of pions and kaons in the mean annihilation (11). Several chains must be considered. This long procedure results in (secondary and successive $\pi^\circ \to 2\gamma$ decays are considered to belong to the step of the mother-particle)

at η decay (1 attosecond after annihilation)

$$M = 715.6 \text{ MeV} \quad KE = 1161 \text{ MeV} \quad GE = 0 \quad NE = 0 \tag{23}$$

at π° decay (220 attoseconds)

$$M = 451.0 \text{ MeV} \quad KE = 722.9 \text{ MeV} \quad GE = 702.7 \text{ Mev} \quad NE = 0 \tag{24}$$

at K_S° decay (0.11 nanoseconds)

$$M = 445.2 \text{ MeV} \quad KE = 726.1 \text{ MeV} \quad GE = 705.3 \text{ MeV} \quad NE = 0 \tag{25}$$

at $K^\pm$ decay (16 nanoseconds)

$$M = 436.1 \text{ MeV} \quad KE = 727.8 \text{ MeV} \quad GE = 707.2 \text{ MeV} \quad NE = 5.5 \text{ MeV} \tag{26}$$

at K_L° decay (66 nanoseconds)

$$M = 431.6 \text{ MeV} \quad KE = 728.3 \text{ Mev} \quad GE = 709.4 \text{ MeV} \quad NE = 7.3 \text{ MeV} \tag{27}$$

at $\pi^\pm$ decay (110 nanoseconds: any charged pion, primary or produced by a kaon decay, is decayed)

$$M = 326.4 \text{ MeV} \quad KE = 586.3 \text{ MeV} \quad GE = 709.4 \text{ MeV} \quad NE = 254.5 \text{ MeV} \tag{28}$$

4.3 Final Products

The last step is represented by the muon decay. Like pions, muons decay at different times because they are produced in different chains as shown in (22). We have electrons, gammas and neutrinos as the final absolutely-stable products after seven microseconds since annihilation. We compute M, KE, GE and NE at this step for completeness.

We should point out that the dominant mode of the μ-decay is

$$\mu^\pm \to e^\pm + 2\nu \tag{29}$$

Another possible channel yields a gamma ray. Very rare modes have been also observed [27]. For our purposes the decay (29) is the only one considered. Several factors intervene, in the rest frame of the muon, in the probability of emission of an electron of a certain energy at a given angle per time unit [10]. However, the mean energy of the emitted electron (or positron) is 0.35 of the muon's mass, or about 37 MeV. Therefore, the neutrinos carry about 68.7 MeV in the muon rest frame. Their mean energies in

LAB are then known (from the LAB energy of the muons) by transforming back and considering a mean value of the parallel-to-muon-speed momentum component equal to zero. Analogous considerations have been made in computing the sets of values (25) through (28).

The mean energies of the muons involved in the last step of the post-annihilation chain decay range from 166 to 331 MeV. Writing the reaction $p + \bar{p} \rightarrow$ (last step) is very long and we omit it here. We give the results of interest as follows

$$M = 1.6 \text{ MeV} \quad KE = 317.9 \text{ MeV} \quad GE = 709.4 \text{ MeV} \quad NE = 847.7 \text{ MeV} \tag{30}$$

The decimals in (23) through (30) are to be intended as round figures for the energy balance in the mean annihilation process considered. The experimental errors propagated in our calculations are greater than a fraction of MeV.

Now we have the necessary elements at hand to plot the energy sharing *versus* time for the products of the $p\bar{p}$ annihilation at rest. Figure 2 displays such behaviour. In Section 8 we will discuss some of the possible or potential implications in propulsion.

5. THE ANTIPROTON-NEUTRON ANNIHILATION AT REST

This section should follow the same guidelines of Section 4. Unfortunately, the statistics in experiments of $\bar{p}n$ annihilation at rest is at present much lower than that of $\bar{p}p$. The results of $\bar{p}n$ annihilation are somewhat different from those relating to the $\bar{p}p$ process. This can be suspected by considering the initial $\bar{p}n$ conditions. First, the total charge is -1; second, the $\bar{p}n$ state is a pure isospin state (equal to one) in contrast to the $\bar{p}p$ system which contains a mix of isospin 0 and 1 [28]. Furthermore, the $\bar{p}n$ annihilations can occur only in nuclei heavier than H. The simplest target in a bubble chamber is then liquid deterium. The $\bar{p}d$ annihilation proceeds through the formation of the antiprotonic deuterium like the protonium in the pure $\bar{p}p$ annihilation. Because the deuteron's binding energy is about 2.2 MeV, a small value, the first reasonable assumption is that the antiproton annihilates on a substantially free neutron, while the proton acts as a "spectator." (This represents the so-called "impulse approximation." The proton carries away its Fermi momentum only [28, 29].

Naturally, in a $\bar{p}d$ reaction $\bar{p}p$ annihilation occur as well. The $\bar{p}n$ process is distinguished from its odd number of prongs. The $\bar{p}n$ annihilation is assumed to take place in S-wave because the only difference in the formation of the antiprotonic deuterium with respect to that of the protonium consists essentially of the Rydberg constant which is scaled up by 4/3. An advantage in analysing $\bar{p}d$ annihilations is to determine the relative $\bar{p}p$ and $\bar{p}n$ annihilation cross sections. From [28] we report

$$\sigma(\bar{p}\text{-}n)/\sigma(\bar{p}\text{-}p) = 0.76 \pm 0.02 \tag{31}$$

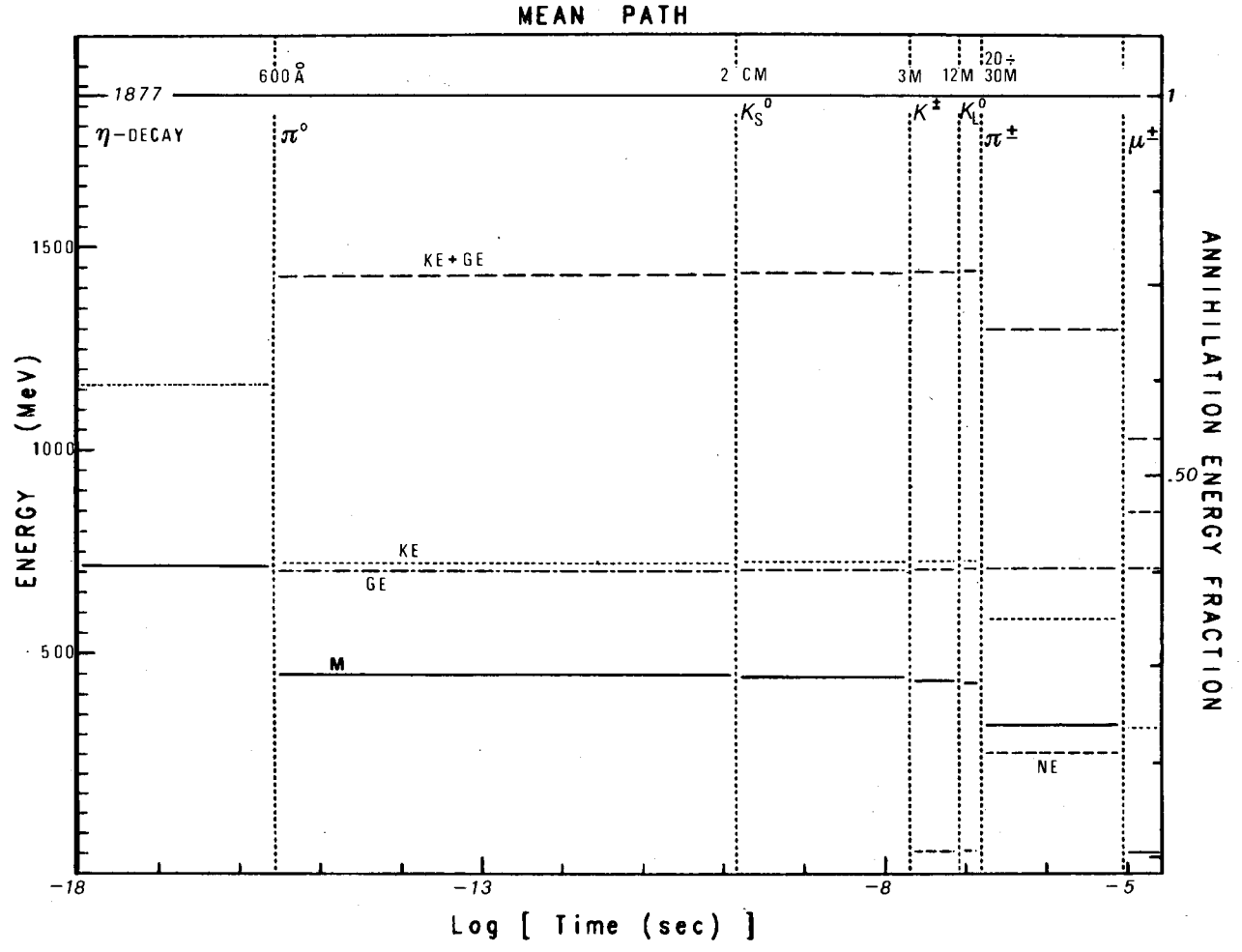

Fig. 2. Proton-antiproton annihilation primary and secondary product mean energy as function of time since the annihilation. Massive particle rest mass (M), kinetic energy (KE), gamma energy (GE) and neutrino energy (NE) are of prime importance in space propulsion applications. Particle fractional energy and meanpath are indicated.

a very important figure when one conceives an antimatter engine where the "annihilation chamber" contains atoms with $A > 1$.

The intermediate states intervening in the $\bar{p}n$ annihilation process are different from the $\bar{p}p$'s. We highlight the major features. Details can be found in Refs. 28-31. As far as the charged pion spectra are concerned, the negative pion energy spectrum is more complex than the positive pion's because two-body intermediate states are present in the reaction $\bar{p} + n \rightarrow \pi^- + (\text{anything})$. They are

$$\bar{p} + n \rightarrow \pi^- + (\rho\rho);\ \pi^- \omega\ ;\ \pi^- + \phi\ ;\ \pi^- + \pi^\circ \qquad (32)$$

Only the first one has been retained here for the π^- mean energy computation because the experimental signals of the other ones are rather feeble. We give the mean energy values of π^+ and π^- after a suitable processing of the fitting momentum distributions given in Ref. 31 as follows:

$$dn_\pi^+/dE = (2SP^2/E)\,(0.057\ m_X^{4.62} + 0.101\ m_X^{1.09}) \qquad (33)$$

$$dn_\pi^-/dE = dn_\pi^+/dE + 0.152\ m_X^{2.76} + Sm_X^{-1/2} + 0.017/[(m_X^{1/2} - 1.51)^2 + 0.011] \qquad (34)$$

where we have set $S = m_p + m_n$ (proton+neutron mass) and $m_X = S^2 - 2SE + m_\pi^2$ · E, P and m_π denote the total energy, momentum and mass of the charged pion, respectively. m_X is the missing mass squared in the reaction $\bar{p} + n \rightarrow \pi + (\text{anything})$.

The last term in Eq. (34) is a Breit-Wigner distribution describing the $(\rho\rho)$ structure of (32). The related mean and width are expressed in GeV. Equations 33-34 are normalised to the mean number of π^+ and π^-, respectively, as observed experimentally through their occurrence frequencies. It is possible, therefore, to obtain by a numerical integration both the averaged values of the number and energy of the charged pions. Furthermore, from Ref. 30 one can carry out the mean number of kaons by the partial rates of the several $(K\bar{K})$ channels of the reaction $\bar{p} + n \rightarrow K\bar{K} + (\text{anything})$. A long estimation procedure has brought us to the following $\bar{p}$-n annihilation at rest process averaged over 0.145 and 0.91 GeV (these figures represent experimental limits) of the total pion's energy:

$$\bar{p} + n \rightarrow 1.067\ \pi^+ + 2.046\ \pi^- + 0.024\ K^\circ + 0.024\ \bar{K}^\circ + 0.029\ K^- + 0.020\ K^+ + x\ \pi^\circ \qquad (35)$$

The conservation of charge is within the eperimental errors in determining the frequencies of the pions and kaons. The 'x' in the neutral pion term means that it has not been possible for us to determine the number of π° starting from the references at our disposal. Only the overall energy of $(x\ \pi^\circ)$ can be estimated, and this is important in propulsion applications. We have obtained the following mean energy figures:

$$E(\pi^+) = 366.4\ \text{MeV} \qquad E(\pi^-) = 379.3\ \text{MeV}$$
$$E(K+\bar{K}) \cong 1220\ \text{MeV} \qquad E(x\pi^\circ) \cong 652\ \text{MeV} \qquad (36)$$

Let us note that the averaged energy of the charged pions is 375 MeV and the value 652 MeV is well within the error in the mean overall π°'s energy in $\bar{p}p$ annihilation. Only the kaons contribution appears outside the corresponding errors, but not excessively. These results, together with the fact that the current $\bar{p}n$ statistics are lower than the $\bar{p}p$'s, induce us to conclude that further investigations are required to understand the nucleon-antinucleon dynamics, this being so from a space propulsion potential application viewpoint.

6. HINTS ABOUT THE ANNIHILATION ON HEAVY NUCLEI

An antimatter propulsion system could exhibit a very broad range of thrust. High-thrust stages may in principle be obtained by annihilating a certain amount of antimatter on a much more massive quantity of matter. This matter can be not forced to consist of hydrogen or deuterium. Depending upon particular engine concepts and/or difficult-to-predict-today technology requirements, the reacting mass may consist of elements heavier than deuterium, perhaps high-A elements. These nuclei provide a dense target for an antiprotonic beam.

An incident antiproton eventually produces annihilation on one of the surface nucleons because it should have a low energy for an effective propulsion utilisation. In fact, one can realistically estimate the range of an antiproton in the nuclear matter supposed to be homogeneous. From Ref. 32 we report

$$\lambda_p \cong 70/\bar{\sigma}\ \text{[fermi]} \qquad (37)$$

where the annihilation cross section $\bar{\sigma}$ is expressed in mbarn. This value is to be considered an average of the $\bar{p}p$ and $\bar{p}n$ annihilation cross sections at the antiproton energy. At kinetic energies less than 20 MeV, $\bar{\sigma}$ would be so high that the penetration depth is a small fraction of the nucleon's diameter. However, the cross section cannot increase beyond a certain value on account of the relative speed between the $\bar{p}$ and any nucleon due to the internal nucleus' motion. Some of the mesons produced in the annihilation, as simmetrically emitted in space, can transfer a significant part of their energy to the spectator nucleons. This might result in the explosion of the nucleus the fragments of which can, in turn, interact significantly with the other nuclei provided their density is sufficiently high. However, the relative frequency of such "fireballs" is estimated about 1-2 per cent of all the annihilations on a nucleus. In any case, these rare events and the more "quiet" annihilations all together can contribute to the sharing of the $(\bar{p}N)$ mass among the atoms of a dense flow which can be exhausted away from the spaceship.

To end these very short hints about such big problems, we recall that when the antiprotons are stopped in a dense high-A material, antiprotonic atoms are formed. They de-excite by Auger electrons and hard X-rays. Such energy is probably not wasted for either the propulsion system or other ship's systems. This fascinating field may be one of the several aspects to be investigated to fully exploit the annihilation energy.

7. LOW-ENERGY ANNIHILATION CROSS SECTION

We have seen that, apart from a non-zero probability of annihilation-in-flight, an annihilation-at-rest passes through the formation of antiprotonic atom (a protonium in the case of annihilation on hydrogen). One of the major differences between nucleon-nucleon and nucleon-antinucleon interactions consists of a much stronger field for the $N\bar{N}$ system. In particular, as soon as the antiproton's wave function overlaps the nucleus appreciably in an antiprotonic atom, one of the consequences of the strong attraction may be a non-negligible deviation of the inverse-velocity law in the annihilation cross section. Needless to say, this would impact upon the design of the "annihilation chamber," at least, in an antimatter powered rocket. The current state of the experimental $\bar{p}p$ annihilation cross section (the $\bar{p}$'s momentum in LAB is the independent variable) can be summarised as follows:

1. the annihilation cross section (σ_{an}) is rather large, greater than the elastic cross section (σ_{el}): $\sigma_{an}/\sigma_{el} \cong 1.8$;

2. σ_{an}, σ_{el} and the total $\bar{p}p$ cross section (σ_t) sometimes display resonances;

3. the relationship $\sigma_{an} = \sigma_t(\bar{p}p) - \sigma_t(pp)$, where $\sigma_t(pp)$ denotes the total elastic pp cross section, furnishes in reality only a crude estimation of σ_{an};

4. in general, at $\bar{p}$ momenta lower than 3 GeV/c but higher than the pion threshold, the annihilation cross section is estimated by subtraction: $\sigma_{an} \cong \sigma_t - \sigma_{el} - \sigma_{inel}$ where σ_{inel} denotes the inelastic $\bar{p}p$ cross section;

5. *no* measurements of any cross section are available *below 300 MeV/c.* Other details about the $N\bar{N}$ cross sections can be found in Refs. 20, 22, 27.

The initial states of antiprotonic atoms are strongly affected by the surrounding ambient field. The fact together with point-5 is of particular importance in an antimatter engine concept. The next annihilation experiments at LEAR will supply an enormous amount of data in gaseous environments and at very low antiproton momenta (perhaps down to 10 MeV/c). It is the opinion of the author that within a few years new results about annihilation dynamics will shed light on the space propulsion application.

8. POTENTIAL APPLICATIONS TO SPACE PROPULSION

In this final section we re-arrange the major data so far obtained. We focus our sttention on the quantitative aspects of the annihilation energetics. In order to render the related figures a ready input for investigations about the rocketship dynamics and technology, performance estimation and so forth, we suitably normalise the annihilation mass-energy history displayed in Fig. 1. We will refer to some of the key-parameters defined in Refs. 33 and 34 for modelling a S/C propulsion system. Because of the context of the present paper, possible effects such as energy re-conversion suggested in Refs. 33 and 34 will not be considered explicitly here. However, for the sake of completeness, we repeat the definitions given for all the cited parameters.

First set of parameters [33]:

ϵ is the fraction of the initial energy (two proton masses if referred to one annihilation) which encompasses both the massive particle kinetic energy and the photon energy. Such a value is relevant to the chain decay stage (CDS), following the annihilation, which is being considered;

ϵ_γ is the fraction of the initial energy appearing as photons. It is relevant to the CDS considered;

ϵ_m represents the fraction of the initial energy resulting in rest mass of the massive particles. It is relevant to the CDS considered;

ϵ_k denotes the fraction of the initial energy going to massive particle kinetic energy. It is relevant to the CDS considered;

s is the fraction of the $(1-\epsilon)$ quantity lost into space (at zero total momentum in the ship frame);

s_γ is the actual fraction of ϵ_γ lost into space (at zero total momentum in the ship frame);

σ is the fraction of $(1-s_\gamma)\,\epsilon_\gamma$ re-converted into controllable massive particles. In other words, it represents the rest mass of these particles. Such a re-conversion (if any) makes available the energy $(1-\sigma)(1-s_\gamma)\,\epsilon_\gamma$ as kinetic energy to be added to ϵ_k. Note that $\sigma = 0$ is equivalent to $s_\gamma = 1$, namely, the gamma energy is completely lost.

Second or alternative set os parameters [34]:

ϵ_t is the total yield of the reaction releasing energy to be utilised. It equals one for an annihilation reaction;

ϵ_e is the ϵ_t fraction in terms of the effective total energy of the *non-negligible interaction* particles, ϵ_e equals ϵ_t only if no negligible-interaction particles are produced;

s' is the fraction of $(1-\epsilon_e)$ lost into space (at zero total momentum in the ship frame);

σ' is the ϵ_e fraction in terms of rest mass of the massive particles. It is composed of two quantities we call σ_{sp} and σ_{ind}, where the subscripts 'sp' and 'ind' stand for 'spontaneous' and 'induced' respectively;

σ_{sp} is the ϵ_e fraction which is by reaction in form of product rest-mass;

σ_{ind} is the ϵ_e fraction which is re-converted in rest mass of massive particles.

Because of the generality of the S/C model dealt with in Ref. 34, no further parameter such as s_γ has been introduced in the second set. When re-conversion was considered, ϵ_e would equal $\epsilon_m + \epsilon_k + (1-s_\gamma)\,\epsilon_\gamma$, namely the total energy of the massive particles plus the gamma energy exploited. The generality and the simplicity of such a three-parameter model [34] is retained. Note that for an antimatter propulsion system s' is either zero or one, independently of the re-conversion process (if any). In Refs. 33-34 it is shown with arguments that go beyond the scope of this paper that the following inter-relationship between the two sets of parameters just defined is of particular importance:

$$1 - \epsilon_k - 2(1-s)(1-\epsilon) - (1-s_\gamma)(1+\sigma)\,\epsilon_\gamma = s' - \epsilon_e(\sigma' + s') \qquad (38)$$

The common value of the two sides of Eq. (38) has a profound impact on the optimal control for the maximum final velocity problem [33-34]. It appears to disclose new aspects of optimal control depending upon very high energy yield reaction propulsion systems such as antimatter thrusters may be.

A very useful index of engine performance is represented by the ideal energy efficiency we denote here by λ. It is defined as follows. If certain energy-carrier particles are to be ejected and, optionally, their energy is shared with an amount of inert matter, then λ is the ratio between the ejection energy and the total energy of the exothermic reactions. It is plain that λ mus be independent of the particular set of parameters selected for a certain mission/propulsion analysis. In the current case it is fundamental to realise that λ is a reaction-dependent value. No similar ideal behaviour has been seen in other propulsion concepts. The fact has been first emphasised quantitatively by Cassenti [6].

TABLE 1.

Particle Decaying Parameter	η	π°	k_S°	$k^\pm$	k_L°	$\pi^\pm$	$\mu^\pm$
ϵ	0.619	0.760	0.763	0.765	0.766	0.690	0.547
ϵ_k	0.619	0.385	0.387	0.388	0.388	0.312	0.169
s	0	0	0	0.012	0.017	0.438	0.998
ϵ_m	0.381	0.240	0.237	0.232	0.230	0.174	0.0009
ϵ_e	1	0.626	0.624	0.620	0.618	0.486	0.170
s'	0	1	1	1	1	1	1
σ_{sp}	0.381	0.384	0.380	0.375	0.372	0.358	0.005
λ		0.626	0.624	0.620	0.618	0.486	0.170

Values of the key parameters at the successive chain decay stages of the proton-antiproton annihilation at rest. The parameter sets are defined in Section 8. The entries can be used in S/C propulsion models [33, 34] to specialise them to antimatter propulsion. No reconversion ($\sigma_{ind} = 0$) is considered here. The corresponding energy efficiency is found in the last row.

TABLE 2.

Particle decaying Parameter	η	π°	k_S°	$k^\pm$	k_L°	$\pi^\pm$	$\mu^\pm$
ϵ	0.619	0.760	0.763	0.765	0.766	0.690	0.547
ϵ_k	0.619	0.385	0.387	0.388	0.388	0.312	0.169
s	0	0	0	0.012	0.017	0.438	0.998
ϵ_m	0.381	0.240	0.237	0.232	0.230	0.174	0.0009
σ	0	0.0029N*					
ϵ_e	1	0.813	0.812	0.809	0.807	0.675	0.359
s'	0	1	1	1	1	1	1
σ_{sp}	0.381	0.296	0.292	0.287	0.285	0.258	0.0024
σ_{ind}	0	0.0007N*				0.0008N*	0.0015N*
λ		0.813	0.812	0.809	0.807	0.675	0.359

The equivalent of Table 1 for 50% photon energy re-conversion. that is $s_\gamma = 0.50$. It is supposed that gammas are converted in high relativistic electron-positron pairs. The undefined N* in the table stands for the mean effective number of pairs (per one annihilation) which may be generated by conversion. Its value depends upon the process used (e.g. an electromagnetic shower).

Here we suggest that his upper limit (pion ejection) can in principle be extended by the concept of energy re-conversion. It is easy to recognise that λ equals ϵ_e as Tables 1-2 report. It will be probably hard to obtain more than one-half of the total gamma energy available in a stage. Therefore, we are induced to deem that the maximum λ ranges from 0.62 to 0.81 whereas the minimum λ lies between 0.17 and 0.36. Noting the strong drop of λ following the decay of the charged pions, one should possibly conceive antimatter propulsion systems such that the characteristic times of ejection or energy transfer are shorter than about 0.1 μsec. In any case, it should be inadvisable to wait for the muon's decay, as it is apparent.

A question arises: what is a favourable characteristic time of ejection? In other words, what would a suitable engine size be for an efficient thruster? Naturally, the question is quite complex, depending upon a high number of parameters of different origin. We wish to hint at an aspect that may be non-negligible in a realistic engine. From Figs. 2 and the above considerations, the charged pions are allowed to have a path of 20 metres. The magnetic nozzle along which the particles move should contain a high magnetic energy density. This can be easier obtained in a small nozzle (in its upper zone the annihilations should occur). There are technological limits interlacing with physical limits, of course. One of these may be determined by the lifetime of k_L°. From a propulsion standpoint the kaon energy contribution could be neglected. However, if the annihilation chamber characteristic size were less than 11-12 metres, every k_L° would impinge upon the structure provided that a high-jet-speed engine is under consideration. In Section 3 we mentioned a minimum order of magnitude of the annihilation rate for a relativistic-specific-impulse engine. . we consider 10^{21} annihilations per second and the values in the mean

reaction (11), the power to be absorbed by the structures amounts to about 1 GW! (taking into account the k°_{L} decay energy, and much more for an interstellar thruster.

Although it is rather difficult to envisage the details of an antimatter-based propulsion system, the point is that a careful analysis of the annihilation outcomes and their impact on the engine design at the different chain decay stages is required.

Several effects would degrade the ideal efficiency. Some of these are foreseeable because they are conceptually similar to those of less exotic propulsion concepts. New effects peculiar to antimatter thrusters are expected. A good goal should be a propulsion system exhibiting an energy efficiency ranging from 0.60 to 0.70. Such a system would be capable of accomplishing complex missions towards the nearby stars [35]. We should add that the overall mass utilisation efficiency – as defined in Ref. 34 in general – would be greater than the energy efficiency if an inert additional mass is given the annihilation energy.

It is well known in the antimatter propulsion community which are the highly challenging fields to be investigated in order to "convert" ideas to practice. It is not an opinion of the author but a fact that examples of major difficulties come from the anti-H production and the control of such antiatoms just formed (they are neutral!). The current high-vacuum technology limits pose other problems on long antimatter storage. Very long storage times – for missions requiring a final deceleration or a more general manoeuvre – will most probably be dealt with by new techniques. Perhaps the new experiments in progress or already planned at CERN may disclose quite unexpected aspects from which key applications may be drawn.

9. CONCLUSIONS

In this paper we have presented a synthesis of the current experimental data about the antiproton-nucleon annihilation at rest. This special review has been oriented towards a possible future application to Astronautics of the great amount of annihilation energy.

We started, very simply, be recalling some of the basic concepts in particle physics and by briefly describing the environments where the experiments on annihilation have so far been performed. We have focussed our attention on the number and energy (or momentum) spectra of the mean-annihilation-at-rest process. We have first dealt with the proton-antiproton annihilation. Subsequently, the antiproton-neutron annihilation has been described, largely in the light of the more general antiproton-nucleus annihilation process which may be a realistic environment in both high-thrust and low-thrust high-efficiency engine designs. The current state of the annihilation cross section experiments has been briefly summarised.

Finally, two sets of parameters useful in examining both antimatter rocket dynamics and the performance of antimatter engines have been defined. These parameters quantify the mass-energy utilisation history that can be built up by starting from the annihilation primary products and then considering their successive multiple decays. Tables or graphs displaying such history (or its equivalent) can be of prime concern for the analysis of antimatter propulsion concepts, especially in engine/mission simulation computer codes.

ACKNOWLEDGEMENTS

The author is very grateful to Prof. R. Bizzarri of the Physics Institute of Rome University for his precious support in suggesting key references, for discussion about the current concepts of annihilation and for reading this manuscript.

Also, particular thanks go to Dr. M. Gaspero for additional information about the results of his paper referenced here.

REFERENCES

1. E. Sanger, "Zur Theorie der Photoneraketen," *Ingenieur Archiv*, **21**, 213 (1953).
2. D. D. Papailou (Ed.), "Frontiers in Propulsion Research," JPL Technical Memorandum 33-722, 1975.
3. B. N. Cassenti, "A Comparison of Interstellar Propulsion Systems," *JBIS*, **35**, 116 (1982).
4. P. F. Massier, "The Need for Expanded Exploration of Matter-Antimatter Annihilation for Propulsion Applications," *JBIS*, **35**, 387 (1982).
5. R. L. Forward, "Antimatter Propulsion," *JBIS*, **35**, 391 (1982).
6. B. N. Cassenti, "Design Considerations for Relativistic Antimatter Rockets," *JBIS*, **35**, 396 (1982).
7. D. L. Morgan,Jr., "Concepts for the Design of an Antimatter Annihilation Rocket," *JBIS*, **35**, 405 (1982).
8. R. R. Zito, "The Cryogenic Confinement of Antiprotons for Space Propulsion Systems," *JBIS*, **35**, 414 (1982).
9. G. Chapline, "Antimatter Breeders?" *JBIS*, **35**, 423 (1982).
10. E. Segrè, "Nuclei and Particles," The Benjamic/Cummings Publishing Company, Reading (Mass.), 1977.
11. M. A. Preston and R. K. Badhuri, "Structure of the Nucleus," Addison Wesley, Reading (Mass.), 1975.
12. R. Omnès, "Introduction to Particle Physics," Addison Wesley, Reading (Mass.), 1971.
13. D. H. Wilkinson (Ed.), "Isospin in Nuclear Physics," North-Holland, Amsterdam, 1969.
14. L. I. Shiff, "Quantum Mechanics," (3rd Edition), McGraw-Hill, New York, 1968.
15. R. Wilson, "The Nucleon-Nucleon Interaction," Wiley-Interscience, New York, 1963.
16. R. E. Marshak and E. C. G. Sudarshan, "Introduction to Elementary Particle Physics," Wiley-Interscience, New York, 1961.
17. R. Feynman, "The Theory of Fundamental Processes," Benjamin Ed., New York, 1961.
18. ASTERIX Collaboration, "A Study of $\bar{p}p$ Interactions at Rest in a H_2 Gas Target at LEAR," proposal of experiment at CERN (Geneva), 1980.
19. E. Klempt, "Antiprotonic Atoms."***
20. M. A. Schneegans, "NN Annihilation at LEAR."***
21. H. Koch, "Investigations on Baryonium with Stopped Antiprotons."***
22. H. R. Rubinstein, "Theory of Nucleon-Antinucleon Annihilation."**
23. R. Armenterous and B. French, "Antinucleon-Nucleon Interactions in High Energy Physics," Academic Press, New York, 1969.
24. CERN-College de France Collaboration, "An Inclusive View on $\bar{p}p=n\pi$ at Rest."**
25. T. Fields and R. Singer, "Clusters in $\bar{p}p$ Annihilation and in pp Pionisation."**
26. C. Defaix and P. Espigat, "Experimental Analysis of the Reaction $\bar{p}p = 2\pi^{+}2\pi^{-}\pi^{\circ}$ at Rest (non ω° events); Evidence for a $\rho^{\circ}\rho^{\circ}$ Effect around 1440 MeV."**
27. "Review of Particle Properties, Particle Data Group," from Physics Letters, **111B**, August 1982.
28. R. Bizzarri *et al.*, "Pion and Kaon Production in Antiproton-Neutron Annihilations at Rest," Il Nuovo Cimento **53A**, 1964.
29. A. Bettini *et al.*, "Annihilations $\bar{p}n$ at Rest into Final States Containing K-mesons," Il Nuovo Cimento, **62A**, 1038 (1969).
30. T. Papadopoulou *et al.*, "The Inclusive Charged Pion Spectra in $\bar{p}n$ Annihilations at Rest," Physics Letters, **43B**, 401 (1973).
31. M. Gaspero, "π^{+} and π^{-} Inclusive Spectra in $\bar{p}n$ Annihilation at Rest," Internal Note 527 of Institute of Physics, Rome University, 1974.
32. J. Rafelski, H. T. Elze and H. Hagerdou, "Hot Hadronic and Quark Matter in $\bar{p}$-Annihilation on Nuclei." ****
33. G. Vulpetti, "An Approach to the Modeling of Matter-Antimatter Propulsion Systems," submitted to *JBIS*, 1983.

34. G. Vulpetti, "A General Formulation of the Maximum Terminal Velocity Problem," in press, *Acta Astronautica.*
35. G. Vulpetti, "Relativistic Astrodynamics: The Problem of Payload Optimisation in a Two-Star Exploration Flight with an Intermediate Powered Swing-by," 34th IAF Congress, IAF-83-327, Budapest, October 1983.

In the above references, the following notation is used:

** = Proceedings of the Symposium on Antinucleon-Nucleon Annihilations, Chexbres, 1972.

*** = Proceedings of the Joint CERN-KFK Workshop on Physics with Cooled Low Energetic Antiprotons, Karlsruhe (West Germany), March 1979.

**** = 5th European Symposium on Nucleon-Antinucleon Interactions, Bressanone (Italy), June 1980.

* * * * * * *